Pairing Correlations in the Two-Dimensional Hubbard Model

Shiwei Zhang

Department of Physics, The Ohio State University, Columbus, OH 43210
Department of Applied Science and Department of Physics, College of William and Mary, Williamsburg, VA 23187 *

J. Carlson and J.E. Gubernatis

Theoretical Division, Los Alamos National Laboratory, Los Alamos, NM 87545
(February 1, 2008)

We present the results of a quantum Monte Carlo study of the extended s and the $d_{x^2-y^2}$ pairing correlation functions for the two-dimensional Hubbard model, computed with the constrained-path method. For small lattice sizes and weak interactions, we find that the $d_{x^2-y^2}$ pairing correlations are stronger than the extended s pairing correlations and are positive when the pair separation exceeds several lattice constants. As the system size or the interaction strength increases, the magnitude of the long-range part of both correlation functions vanishes.

PACS numbers: 74.20.-z, 71.10.Fd, 71.10.-w, 02.70.-c

Since the discovery of high-temperature superconductivity, the two-dimensional Hubbard model has been the subject of an unprecedented level of theoretical activity to discover whether it can serve as the paradigm for this novel and important phenomenon. Particularly with respect to magnetic properties [1], the physics of the model qualitatively represents the behavior of the real materials. For example, at half-filling the model is an anti-ferromagnetic insulator. Upon doping the anti-ferromagnetism rapidly becomes strongly suppressed. This behavior is observed in the cuprate superconductors. A variety of calculations also predict [2] that the doped model exhibits an attractive interaction between pairs; the s and $d_{x^2-y^2}$ symmetries of this attraction are consistent with the likely symmetries of the experimentally measured superconducting gap [2]. Yet unobserved, however, is convincing evidence that the attractive interaction leads to a ground state with off-diagonal long-range order [1,2]. In this paper we will present results from quantum Monte Carlo (QMC) simulations which suggest that the long-range extended s and $d_{x^2-y^2}$ pairing correlations in fact vanish in the thermodynamic limit.

The fundamental difficulty in deciding whether the two-dimensional Hubbard model superconducts is the absence of an exact solution. Approximate solutions have often been uncontrolled, difficult to benchmark, and conflicting. On several key points, computer simulations have provided important information. In fact, the possible existence of superconductivity in the Hubbard model was suggested by the results of a QMC simulation before the discovery of the high temperature superconducting materials [3].

Numerical approaches have, however, had their own difficulties, typically being limited to small system sizes, high temperatures, and selected electron fillings. Quantum Monte Carlo methods, for example, experience the infamous fermion sign problem [4,5], which causes an exponential growth in the variance of the computed results and hence an exponential growth in computer time as the lattice size is increased and the temperature is lowered. While QMC simulations have shown indications of pairing correlations, uncertainty has remained because of their restriction to relatively small lattice sizes and high temperatures [2,6].

Here, using our new constrained path Monte Carlo (CPMC) method [7], we discuss the behaviors of the extended s and $d_{x^2-y^2}$ pairing correlations obtained from simulations free of such restrictions. Contrary to standard algorithms [8,9], this new ground-state ($T = 0$ K) method exhibits *algebraic* scaling of computer time with system size. It eliminates the exponential growth of variances by what we call the constrained-path approximation. In a variety of benchmarking calculations [7], the CPMC method has yielded accurate estimates of the energy as well as other ground-state observables.

We considered the following familiar form of the two-dimensional Hubbard model on a square lattice of $N = L \times L$ sites with N_σ ($\sigma = \uparrow, \downarrow$) electrons:

$$H = -t \sum_{\langle ij \rangle \sigma} (c_{i\sigma}^\dagger c_{j\sigma} + c_{j\sigma}^\dagger c_{i\sigma}) + U \sum_i n_{i\uparrow} n_{i\downarrow}. \qquad (1)$$

we took $t = 1$ and assumed periodic boundary conditions. The pairing correlation function we computed is

$$P_\alpha(l) = \langle \Delta_\alpha^\dagger(l) \Delta_\alpha(0) \rangle, \qquad (2)$$

where α indicates the nature of pairing. The pair field-operator at site l is $\Delta_\alpha(l) = \sum_\delta f_\alpha(\delta)[c_{l\uparrow} c_{l+\delta\downarrow} - c_{l\downarrow} c_{l+\delta\uparrow}]$, where δ is $(\pm 1, 0)$ and $(0, \pm 1)$. For extended s pairing, $f_s(\delta) = 1$. For $d_{x^2-y^2}$ pairing, $f_d(\delta)$ is 1 when $\delta = (\pm 1, 0)$ and -1 otherwise.

To facilitate contact with prior simulations, we also examined the "vertex contribution" to the correlation function [8] defined by

$$\bar{P}_\alpha(l) = P_\alpha(l) - \langle\Delta_\alpha^\dagger(l)\Delta_\alpha(0)\rangle_0 \qquad (3)$$

The second function on the right is shorthand notation for the uncorrelated pairing correlation. For each term in $P_\alpha(l)$ like $\langle c_\uparrow^\dagger c_\uparrow \, c_\downarrow^\dagger c_\downarrow\rangle$, it has a term like $\langle c_\uparrow^\dagger c_\uparrow\rangle\langle c_\downarrow^\dagger c_\downarrow\rangle$.

Our numerical method is extensively described and benchmarked elsewhere [7]. Here we only discuss its basic approximation. In this method, the ground-state wave function $|\Psi_0\rangle$ is projected from a known initial wave function $|\Psi_T\rangle$ by a branching random walk in an overcomplete space of Slater determinants $|\phi\rangle$. In such a space, we can write $|\Psi_0\rangle = \sum_\phi \chi(\phi)|\phi\rangle$, where $\chi(\phi) > 0$. The random walk produces an ensemble of $|\phi\rangle$, called random walkers, which represent $|\Psi_0\rangle$ in the sense that their distribution is a Monte Carlo sampling of $\chi(\phi)$.

To completely specify the ground-state wave function, only determinants satisfying $\langle\Psi_0|\phi\rangle > 0$ are needed; hence, $|\Psi_0\rangle$ resides in either of two degenerate halves of the Slater determinant space, separated by a nodal plane $\mathcal{N}$ that is defined by $\langle\Psi_0|\phi\rangle = 0$. The sign problem occurs because walkers can cross $\mathcal{N}$ as their orbitals evolve continuously in the random walk. Asymptotically they populate the two halves equally, leading to an ensemble that has zero overlap with $|\Psi_0\rangle$. If $\mathcal{N}$ were known, we would simply constrain the random walk to one half of the space and obtain an exact solution of Schrödinger's equation. Without *a priori* knowledge of $\mathcal{N}$, we use a trial wave function $|\Psi_T\rangle$ and require $\langle\Psi_T|\phi\rangle > 0$. The random walk again solves Schrödinger's equation in determinant space, but under an approximate boundary-condition. This is what we call the constrained-path approximation.

The ground-state energy computed by the CPMC method is an upper bound. The quality of the calculation clearly depends on the trial wave function $|\Psi_T\rangle$. Since the constraint only involves the overall sign of its overlap with any determinant $|\phi\rangle$, it seems reasonable to expect the results to show insensitivity to $|\Psi_T\rangle$. Through extensive benchmarking on the Hubbard model, we have found that simple choices of this function can give very good results [7]. In the calculations reported here we took $|\Psi_T\rangle$ to be a single Slater determinant. For closed-shell electron fillings, we used the free-electron ($U = 0$) wave function. For open-shell fillings, we used unrestricted Hartree-Fock (uHF) solutions. For the latter, we have found that uHF solutions obtained with low U values (< 1), i.e., those resembling free-electron wave functions, tend to be good choices for $|\Psi_T\rangle$ for U up to 8.

As a calibration of our method, we compare in Table 1 its prediction for the $d_{x^2-y^2}$ pairing correlation function to that obtained by an exact diagonalization calculation [10] of a 4×4 lattice with a closed shell filling of $N_\uparrow = N_\downarrow = 5$ and with $U = 2$ and 4. At each location of the pairs, we reproduce the exact result within an error of 1 % or less. (Here, in order to compare with the exact diagonalization data we computed $\langle\Delta_d(l)\Delta_d^\dagger(0)\rangle$ with

$$\Delta_d(l) = c_{l\uparrow}\sum_\delta f_d(\delta)c_{l+\delta\,\downarrow}.)$$

As a further calibration of our method, we show in Fig. 1 the long-range portion of the $d_{x^2-y^2}$ pairing correlation $P_d(l)$ as a function of $|l|$ for a half-filled 8×8 system at $U = 4$. At half-filling, the standard auxiliary-field quantum Monte Carlo (AFQMC) method [9] has no sign problem and is exact, and the CPMC method can be made exact by removing the constrained path condition. In this CPMC calculation, however, we deliberately kept the constraint and used for $|\Psi_T\rangle$ the uHF solution of the system at $U = 0.5$. In the figure, the computed $P_d(l)$ from the CPMC simulation is compared with exact AFQMC results. Also shown is the result predicted by $|\Psi_T\rangle$. The inset shows, as a function of electron filling $(N_\uparrow + N_\downarrow)/N$, the relative difference between the ground-state energies calculated by CPMC and AFQMC simulations. The point indicated by the arrow corresponds to the CPMC calculation shown in the main graph. At 1%, this difference represents the largest systematic error in the CPMC calculation of the energy. With the energy as a gauge, the CPMC calculation at 1/2-filling would appear to be of the poorest quality; yet, we see that it still yields an accurate $P_d(l)$. The magnitude and range of these correlations is comparable to those we now discuss for the doped cases.

Figure 2 shows the long-range part of $P_d(l)$ as a function of $|l|$ for a 12×12 lattice at $U = 2$, 4, and 8. Here, the electron filling is 0.85, which corresponds to a closed shell case with $N_\uparrow = N_\downarrow = 61$. Figure 2a, the $U = 2$ case, shows three different evaluations of this correlation function. One is the free-electron prediction for the pairing. Another is based on definition (2), and the third is the vertex contribution to this definition. Figure 2b shows the same set of curves for $U = 4$ while the inset to Figure 2b shows the $U = 8$ results with the vertex contribution omitted for clarity. These three sets of curves show that $P_d(l)$ is smaller at all three vaules of U than the non-interacting case. They also show that increasing U causes the long-range correlations, including the vertex contribution, to vanish. At $U = 8$, despite the large error bars, the correlations are reduced to simply fluctuating around zero. We also see that the vertex contribution is a fairly flat function of pair separation up to $U = 4$. This flat region is the "plateau" observed in Ref. [11] for calculations up to $U = 2$. In this work the Hubbard model was studied with next near-neighbor hopping and the existence of the "plateau" was attributed to its presence. Our results show that the "plateau" behavior is no less pronounced in the simple Hubbard model. As U increases to 8, however, it vanishes as $P_d(l)$ does.

In Fig. 3, we address the question of what happens to these "long-range" correlations if the lattice size is increased to 16×16. Here, for a closed shell case with the same electron filling of 0.85 ($N_\uparrow = N_\downarrow = 109$), we show the CPMC results for $U = 2$ and 4. First, we notice that as in Fig. 2 increasing interaction strength eventu-

ally causes the correlations to vanish but now they vanish by $U = 4$. The $U = 4$ case is shown in Fig. 3b; the accuracy is still sufficient to discern the irregular oscillations of $P_d(l)$ around zero. In Fig. 3a the vertex contribution is again relatively flat, but nearly zero. Compared to Fig. 2a, it has decreased with the increase in lattice size. At $U = 4$ it has in fact vanished and it not shown for clarity. We note that we have also carried out calculations with a second neighbor hopping and did not find any qualitatively different behavior.

A representative result for the extended s pairing correlation function $P_s(l)$ is shown in Fig. 4 for the same system as in Fig. 2. The pairing correlation function is shown for the whole range of $|l|$. Its short-distance magnitude is much greater than that in the tail. We mention that the $d_{x^2-y^2}$-wave pairing correlation shows the same general behavior. In both cases, the short-range correlation actually increases as U is increased from zero. Hence, the often used integrated pairing correlation function, or equivalently the $\mathbf{k} = (0,0)$-component of P_α in momentum space, is *not* a good indicator of superconductivity. Comparing the inset with Fig. 2b, we see that the long-range extended s-wave pairing is at least an order of magnitude weaker than the $d_{x^2-y^2}$ pairing. Indeed it is already fluctuating around zero.

We also studied pairing correlation functions for other electron fillings, lattice sizes, and interaction strengths. These results re-enforce those represented above and will be reported elsewhere. For example, at open-shell fillings, even though the calculations experience significant increases in variances due to a poorer $|\Psi_T\rangle$'s, results through 12×12 systems do not appear to show any significant changes compared to the closed-shell ones.

We reiterate that, due to the constrained-path approximation, the correlation functions computed here are approximate. While the systematic error appears small when compared with exact diagonalization and exact QMC results, we cannot exclude the possibility that as the lattice size increases our systematic error increases and an underestimation of the correlations develops. By the same token we cannot exclude overestimation. However, results like those in Table 1 and Fig. 1, plus a variety of other benchmarks [7], indicate that our systematic error is typically small. In fact, it is often orders of magnitude smaller than the statistical error in simulations using the standard AFQMC method.

With this very small statistical error, we have pulled pairing correlations "out of the noise," and have shown examples that for a given system size they disappear as the interaction strength increases and for a given interaction strength they disappear as the system size increases. We note that similar behavior exists for the non-interacting problem and the half-filled case.

We have also computed the lattice size, interaction strength, and electron filling dependence of the ground state energy, electron momentum distribution, and static spin-spin correlation function. We will report these results elsewhere.

*   Present address.

[1] For example, see A. P. Kampf, Phys. Reports **249**, 219 (1994).

[2] See, for example, D. J. Scalapino, Phys. Reports **250**, 329 (1995); in *Perspectives in Many-Body Physics*, edited by R. A. Broglia, J. R. Schrieffer, and P. F. Bortignon (North-Holland, Amsterdam, 1994), pg. 95.

[3] J. E. Hirsch, Phys. Rev. Lett. **54**, 1317 (1985).

[4] K. E. Schmidt and M. H. Kalos, in *Applications of the Monte Carlo Method in Statistical Physics*, ed. by K. Binder (Springer Verlag, Heidelberg, 1984).

[5] E. Y. Loh Jr., *et al.*, Phys. Rev. B **41**, 9301 (1990).

[6] A. Moreo and D. J. Scalapino, Phys. Rev. B **43**, 8211 (1991); A. Moreo, Phys. Rev. B **45**, 5059 (1992).

[7] Shiwei Zhang et al., Phys. Rev. Lett. **74**, 3652 (1995); Phys. Rev. B, to be published.

[8] S. R. White, et al., Phys. Rev. B **39**, 839 (1989).

[9] For example, E. Y. Loh, Jr. and J. E. Gubernatis, in *Electronic Phase Transitions*, edited by W. Hanke and Yu. V.Kopaev (North-Holland, Amsterdam, 1992).

[10] A. Moreo, private communication.

[11] T. Husslein, et al., unpublished.

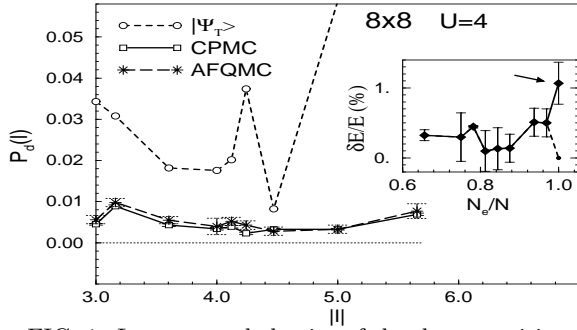FIG. 1. Long-range behavior of the $d_{x^2-y^2}$ pairing correlation function versus distance for a half-filled 8×8 lattice at $U = 4$ computed with $|\Psi_T\rangle$ and by the CPMC and AFQMC methods. The inset shows the relative difference between the CPMC and AFQMC energies as a function of electron filling. The error bars are statistical in origin and mainly associated with the AFQMC results.
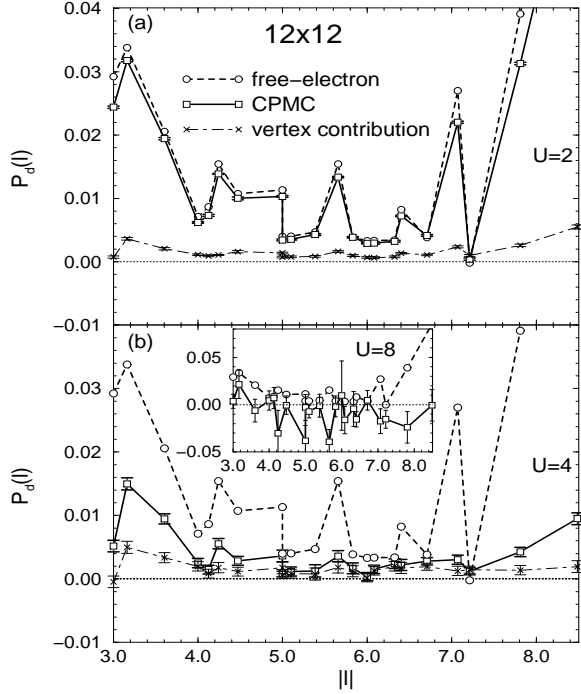

FIG. 2. Long-range behavior of the $d_{x^2-y^2}$ pairing correlation function versus distance for 0.85 filled 12×12 lattice at $U = 2$, 4, and 8. This behavior is shown for the free-electron and CPMC calculations. Also shown is the vertex contribution.

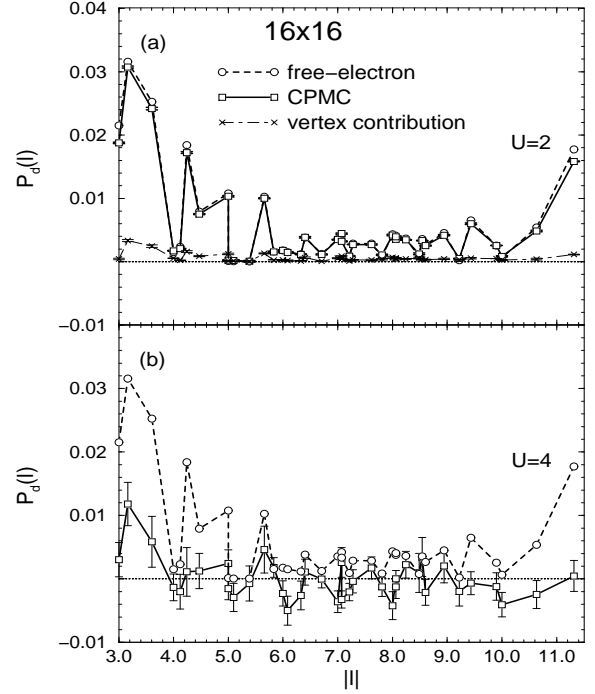FIG. 3. Long-range behavior of the $d_{x^2-y^2}$ pairing correlation function versus distance for a 0.85 filled 16×16 lattice at $U = 2$ and 4. This behavior is shown for the free-electron and CPMC calculations. Also shown is the vertex contribution.

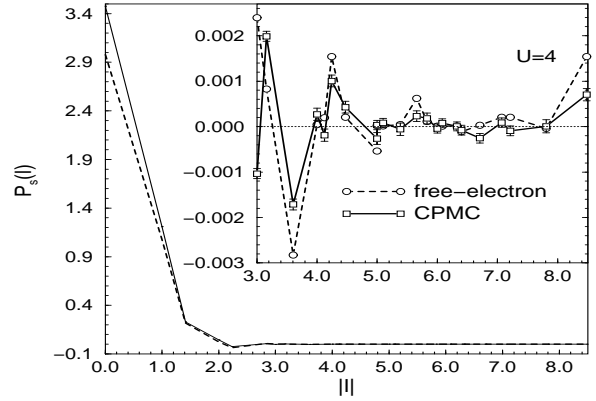FIG. 4. Extended s pairing correlation function versus distance for a 12×12 lattice at $U = 4$ with an electron filling of 0.85. The inset shows long-range behavior of the free-electron case compared with the CPMC result.

TABLE I. Comparison of the CPMC $d_{x^2-y^2}$ pairing correlation function with exact diagonalization results [10] as a function of pair separation $l = (l_x, l_y)$. The system size is 4×4 with $N_\uparrow = N_\downarrow = 5$. In the CPMC calculations the free-electron wave function was used for $|\Psi_T\rangle$. Statistical errors in these calculations are in the last digit and are indicated in parentheses.

U		$(0,0)$	$(1,0)$	$(2,0)$	$(1,1)$	$(2,1)$	$(2,2)$
2	CPMC	2.0672(2)	0.0924(1)	$-0.1121(1)$	0.1140(1)	0.0284(1)	0.1779(2)
	exact	2.06693	0.09223	-0.11187	0.11381	0.02840	0.17793
4	CPMC	2.0635(5)	0.0876(3)	$-0.0941(3)$	0.1006(4)	0.0246(2)	0.1532(6)
	exact	2.06345	0.08714	-0.09422	0.10013	0.02453	0.15302